A Model for Predicting Stroboscopic Flicker

Andrew Bierman, MS, LC

Lighting Research Center, Rensselaer Polytechnic Institute, 21 Union St., Troy, NY 12180

Abstract

One of the many benefits of solid-state lighting is the fast response time of LEDs that enable flexible, precise and efficient electronic control. The downside is that with such a fast temporal response, LED sources have the potential to noticeably flicker and create stroboscopic effects and other undesirable transient light artifacts (TLA). A linear systems model and calculation method for the human detection of stroboscopic TLA is presented. As a first step, the method takes into account the physical characteristics of the object being viewed (size, shape, reflectance, speed) in addition to the temporal characteristics of the illuminating or self-luminous light to determine the physical image stimulus presented to the observer. Then, a model of human contrast perception is applied to quantify the stimulus in terms of a visibility detection threshold.

Predictions of detectable TLA agree well with experimental results and indicate that detection of modulated light is highly variable depending on the exact conditions being viewed. Optimal object profiles and speeds were determined for “worst case” sensitivity to TLA. Surprisingly, this analysis shows that the potential for TLA is independent of light source flicker frequency unless an upper bound is placed on the speed of objects or eye movements. Furthermore, different light source temporal wave shapes maintain the same ranking over a broad range of object conditions and light frequencies thereby indicating that certain wave shapes are less prone to TLA than others for equal percent flicker. A sample ranking from greatest TLA potential to least is square wave, sine, rectified sine, rectangular 20% or 80% duty cycle, ramp, and sawtooth.

Introduction

One of the many benefits of solid-state lighting is the fast response time of LEDs that enable flexible, precise and efficient electronic control. The downside is that with such a fast temporal response, LED sources have the potential to noticeably flicker and create stroboscopic effects and other undesirable transient light artifacts (TLA). LED driver characteristics (frequency, modulation amount, wave shape) determine the potential for TLA, so whether or not TLA is a problem is under the complete control of the driver circuit designer. However, circuit designers need to balance many competing demands such as efficiency, cost, size constraints, and dimming capabilities among others. Therefore, understanding the detection limits of TLA is necessary for optimizing LED driver performance and the acceptability of products brought to market.

Modulated light output is not unique to LED products. Traditional light sources, including incandescent, fluorescent, and high intensity discharge, all have had issues with flicker. The difference with LED sources is that the range of modulation and wave shape is virtually unlimited while traditional light sources of a particular type tended to have similar flicker characteristics and solutions to flicker problems could, therefore, be specific to the technology. For example, the Flicker Index (Eastman and Campbell 1952) was a metric developed for

fluorescent lamps. It did not need to consider frequency as an input variable because all fluorescent lamps operated on 50/60 Hz mains voltage had similar light output frequencies and wave shapes. The IEC flickermeter (IEEE 2010) is another example of a metric developed for a particular lighting technology, general service incandescent lamps, to address flicker problems. The recent publication, "IEEE Recommended Practices for Modulating Current in High-Brightness LEDs," (IEEE 2015) contains a recent review and bibliography of research and metrics concerning light source flicker, however, there is presently little guidance on how to evaluate modulated light output of arbitrary wave shape for the perception of stroboscopic effects.

Flicker can be categorized into three types depending on its effects on people. For frequencies less than about 80 Hz flicker is directly observable as a temporal variation of brightness. Detection of this type of flicker response is well characterized by the ASSIST Flicker Metric (M_P) (ASSIST 2015), as well as an adapted version of the IEC flickermeter published by NEMA (2017). This type of flicker is considered unacceptable for lighting applications and its presence usually indicates poor product quality, a malfunction or incompatibility of lamps and driver equipment. For frequencies between roughly 50 and 200 Hz the term "invisible flicker" (IEEE 2015) is used to describe the subconscious detection of flicker that causes headaches and malaise for a small portion of the population. For frequencies typically above 100 Hz the detection of flicker is made possible by the stroboscopic effect. Detection of the stroboscopic effect is the topic of this paper. It is important for LED lighting applications because many LED products are intentionally designed to modulate light output at frequencies from 100 Hz to several kHz leading to stroboscopic effects and TLA readily produced by the interaction of the modulated light with commonly encountered moving objects.

As opposed to directly perceived flicker, stroboscopic effects are not revealed by the detection of temporally fluctuating light signals, but rather by the conversion of temporal fluctuations into spatial patterns. Therefore, the perception of stroboscopic flicker depends on the detection of spatial contrast which is a fundamentally different visual perception than temporal flicker. Consequently, the visual characterization of stroboscopic flicker must ultimately involve spatial contrast.

In the course of evaluating light sources for potential stroboscopic phenomena one must realize that spatial contrast produced by a flickering light source cannot be assessed by consideration of only the temporal waveform of the light source itself. Rather, one must consider, in addition to the light source, its movement and size (i. e., visual angle) or the movement, size, and reflectance of objects that it illuminates if not directly viewed. In this regard stroboscopic flicker is analogous to color rendering; evaluation of color rendering requires that an object or objects with particular spectral reflectance be specified in addition to the spectral power distribution of the light source itself. Likewise, for evaluating stroboscopic effects a moving stimulus must be defined in addition to the temporal waveform of the light source.

A methodology for quantifying the detection of stroboscopic effects from modulated light sources is presented in this paper. First, the equations for calculating the resulting spatial contrast produced by the interaction of stimulus movement and temporal light modulation are derived. This is purely a physical description of the stimulus presented to the observer which

has been mostly ignored in the literature on flicker and TLA. Second, a linear systems approach is used to apply the human sensitivity for detecting spatial contrast to the physical spatial contrast presented to the observer in order to determine the visibility of stroboscopic phenomena. Finally, predictions from the method are compared to empirical results from previously published studies as well as new data from a human subject experiment designed to test the predictive accuracy of the metric.

Model development

The movement of a temporally varying luminous object within the field of view of an imaging device results in a transformation of temporal variation to spatial variation. This transformation is analogous to the way rapidly fluctuating electrical events are revealed as easily seen waveforms on an oscilloscope screen. To start the analysis, consider Figure 1 which depicts a one-dimensional reflective line moving horizontally across a dark background with a velocity **v** (e. g., 4 m/s). The line is illuminated by a modulated light source having frequency f_{Light} (e. g., 100 Hz), and viewed by an observer at a distance, d (e. g., 4 m). To the observer the light source appears to have a steady light output because 100 Hz is above the critical flicker fusion frequency. As the line moves across the observer's field of view, however, the perception is not of a steadily moving object, but rather a series of bright lines fixed in space. The spacing of the lines is given by the product of the velocity and the frequency of the light modulation (velocity × (1/time) = displacement). In terms of visual angle, the small angular approximation tangent(θ) ≈ θ is used to arrive at a simple expression for the spatial frequency, $f_{Spatial}$, of the resulting stimulus.

$$f_{spatial} = \frac{f_{Light} d}{v} \qquad \text{Equation 1}$$

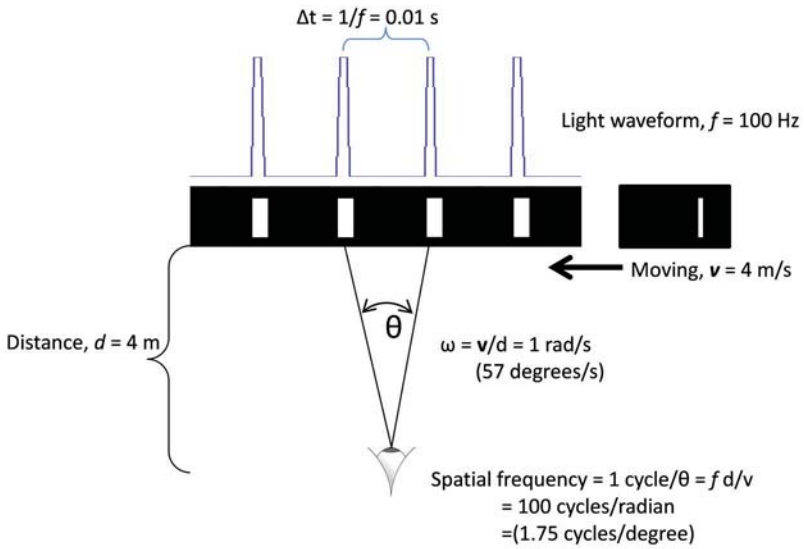

Figure 1. Schematic diagram depicting how a moving object is revealed to an observer as a spatial contrast pattern when viewed under a modulated light source. The production of a spatial contrast pattern in this manner is called a stroboscopic effect.

The simple analysis leading to Equation 1 only provides the frequency of the spatial pattern. To more fully describe the spatial irradiance pattern produced on an imaging detector it is necessary to consider the waveform shape of the temporally modulated light, as well as the shape profile of the reflectance of the moving object. Also, for imaging systems it is more convenient to express dimensions and velocities in terms of visual angle rather than actual distances because visual angle is invariant with viewing distance. Physical modeling of the physical stroboscopic effect has been done previously by Ku et al. (2015) who derived integral equations to model the superposition of reflected light over the exposure duration. While the end result is the same, the analysis here follows a linear systems approach that facilitates computations of complex stimuli and, as described later, enables the perceptual response of the human visual system to be applied as a frequency dependent spatial filter.

The light waveform shape is a function of time, *flux(t)*, and the object can be described by its reflectance profile as a function of position, *o(x)*. As shown in Figure 1, movement of the object reveals the temporal variation of light flux as a spatial variation. We can account for this mathematically by multiplying the time dependency by velocity thereby converting the dependency of flux on time to a variation of flux with distance and ultimately visual angle. Similarly for the object reflectance profile, which is already a function of distance, we can express the object in terms of visual angle.

Light waveform: $l(t) \Rightarrow l(tv) = l(x) \Rightarrow l\left({}^{x}/_{d}\right) = l(\theta_V)$ Equation 2a

Object profile: $o(x) \Rightarrow o\left({}^{x}/_{d}\right) = o(\theta_V)$ Equation 2b

With these conversions both the object profile and the light variation are expressed as functions of visual angle. The resulting contrast pattern presented to the observer is the product of illumination and reflectance at all locations, but because the reflective object is moving superposition of flux occurs over the time interval during which the perceptual image formed. This superposition of light and object reflectance is accomplished mathematically by a convolution. A convolution is a mathematical operation pictured as the result of sliding one function over another while integrating the product of the two over all points. The resulting profile takes on characteristics of both functions. Equation 3 shows the convolution of the light waveform with the object reflectance profile resulting in a stationary physical variation of light intensity with visual angle, i.e. a visual stimulus.

$$\text{Physical stimulus}(\theta_V) = (l * o)(\theta_V) \qquad \text{Equation 3}$$

Equation 3 is a one-dimensional spatial description of the contrast pattern presented to an observer. When velocity is constant this one dimensional analysis is sufficient for characterizing the two-dimensional visual stimulus by constructing it from multiple parallel line profiles. Only in cases of significant acceleration (linear or centripetal) would a more complicated model be needed.

Using a linear systems approach, the perceived visual stimulus is modeled by convolution of the physical stimulus with the spatial impulse response of the visual system. Also, the time response of the visual system needs to be considered as it relates to the persistence of vision that enables the superposition of flux to buildup and form an image. The persistence of vision is

simply modeled as a window in time over which the convolution integral described by Equation 4 is evaluated.

$$\text{Perceptual Stimulus} = ([(l * o)(\theta_V)] * \{\text{Perceptual Impulse Response}\})(\theta_V) \quad \text{Equation 4}$$

The time window is applied by point-by-point multiplication of the object profile, $o(\theta_V)$, by the window profile. A simple exponential decay window with a time constant of 45 milliseconds was used throughout the analysis presented in this paper.

Unfortunately the complete perceptual impulse response of the visual system is not known. However partial information of the perceptual impulse function is well known as the contrast sensitivity function (CSF) and it is readily measured experimentally (Olzak and Thomas 1985). The CSF is the magnitude response of the visual system to luminous spatial contrast as a function of frequency. In preparation for using the CSF Equation 4 is transformed to the spatial frequency domain via a Fourier transform leading to Equation 5.

$$\text{Perceptual Stimulus}(\text{j}\omega) = (L(\text{j}\omega)O(\text{j}\omega))\{\text{Perceptual Impulse Response}\}(\text{j}\omega) \quad \text{Equation 5}$$

The CSF is measured and applied in terms of contrast, so the physical stimulus must also be expressed in terms of contrast. A Weber contrast is obtained by dividing the physical stimulus by the average stimulus intensity which is equivalent to dividing by the zero-frequency component (dc component) as written in Equation 6.

$$C(j\omega) = \frac{|L(\text{j}\omega)O(\text{j}\omega)|}{|L(0)O(0)|} \quad \text{Equation 6}$$

Finally, the magnitude of the perceptual stimulus (ignoring phase) is found by expressing Equation 5 in terms of contrast as defined by Equation 6. The result is given by Equation 7.

$$\text{Perceptual Stimulus}(\omega) = C(\omega)CSF(\omega) \quad \text{Equation 7}$$

If the visual system approximates a linear system then a measure of total spectral power over all spatial frequencies of the stimulus should be given by the quadrature sum of spectral components. Furthermore, if the CSF is provided in absolute units of 1/(contrast needed for detection) then a measure of perceptual stimulus strength is given by Equation 8.

$$\text{Magnitude of Perception} = |C_P(\omega)| = \sqrt[2]{\sum_{i\neq 0} C_{Pi}} \begin{cases} < 1 & \text{not visible} \\ = 1 & \text{just visible} \\ > 1 & \text{visible} \end{cases} \quad \text{Equation 8}$$

A value of 1 for Equation 8 corresponds to a stimulus at the threshold of detection while values less than 1 are not detectable and values greater than 1 are detectable with increasing probability as the value increases.

The experiment described in the next section tests the hypothesis that this modeling of contrast detection using a linear systems approach is predictive of people detecting stroboscopic effects when moving objects are illuminated by modulated light.

Experiment to verify model

Contrast sensitivity functions of eight human observers were measured and then used to predict the detection thresholds of stroboscopic effects from a spinning sector disk illuminated by modulated light of varying wave shapes. Detection thresholds for the several different wave shapes were also measured and compared to the predicted values.

Apparatus

An LED illumination system was built to provide precisely modulated light waveforms for illumination of the visual target and background. It employed a 5000 lumen chip-on-board LED package (Bridgelux, model BXRA, 4100 K) mounted to an aluminum heatsink with a conical aluminum reflector. The LED was driven by a precision voltage-to-current linear amplifier. A direct digital synthesized (DDS) function/arbitrary waveform generator (Agilent, Model 33220A) provided a voltage waveform to the amplifier. The function generator was used in its arbitrary waveform mode whereby digital waveforms from a personal computer were loaded into its memory and used to generate the output waveform. The waveforms used in the study are listed in Table 1.

A custom computer program was written in a high-level development environment (National Instruments, LabVIEW) to generate the digital waveforms, control the presentation of waveforms to the subjects, and provide an interface to collect data from the subjects.

A spinning sector disk provided a moving object for the appearance of stroboscopic manifested flicker. The sector disk was 28 cm in diameter and had eight high reflectance sectors (reflectance factor, $\rho = 0.93$) on a black background ($\rho = 0.06$). Each sector had a width of 2.87 degrees, starting 9 cm from the center of the disk and extending to the edge of the disk. A white screen ($\rho = 0.90$) was placed behind the disk subtending a visual angle of approximately 60 degrees. The sector disk was rotated at a constant angular velocity of 2700 degrees/s (7.5 revolutions/s) by a stepper motor. The LED illumination system provided 300 lux incident on the spinning disk and background. The apparatus is pictured in Figure 2.

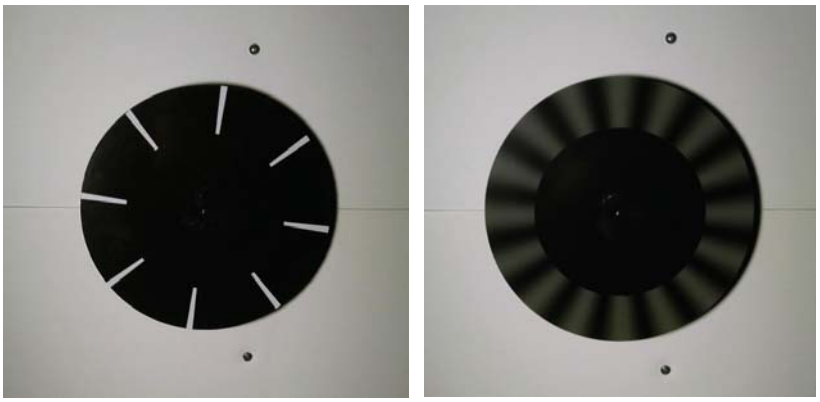

Figure 2. Photograph of the sector disk when stationary (left) and spinning (right).

Table 1. Light waveforms used to illuminate the spinning sector disk.

Waveform type	Frequency (Hz)	Duty cycle (%)	Example
Sine	60	--	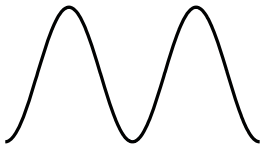
Sine	120	--	
Sine	240	--	
Sine	480	--	
Sine	720	--	
Sine	1380	--	
Sine	2340	--	
Sine	3300	--	
Rectangular	120	10	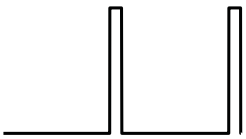
Rectangular	420	10	
Rectangular	1500	10	
Rectangular	60	20	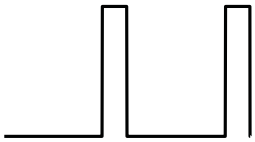
Rectangular	120	20	
Rectangular	240	20	
Rectangular	480	20	
Rectangular	720	20	
Rectangular	1380	20	
Rectangular	2340	20	
Rectangular	3300	20	
Rectangular	120	50	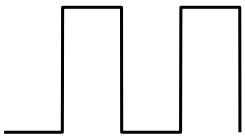
Rectangular	420	50	
Rectangular	1500	50	
Rectified sine	100	--	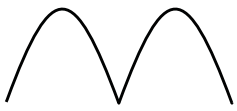
Rectified sine	120	--	
Rectified sine	420	--	
Rectified sine	1500	--	
Sawtooth	120	--	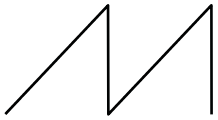
Sawtooth	420	--	
Sawtooth	1500	--	
Ramp (triangle)	120	--	
Ramp (triangle)	420	--	
Ramp (triangle)	1500	--	

Stimulus presentation

A double random staircase method (Cornsweet 1962) was used to determine the detection threshold of each waveform condition shown to the subjects. One staircase began with a clearly visible stroboscopic contrast pattern on the spinning sector disk, while the other began at an undetectable contrast level. Positive contrast identification resulted in a decrease in modulation of the illuminating waveform for the next presentation of that staircase and negative responses resulted in a modulation increase. To avoid presenting learnable patterns of modulation, presentations of the two staircases were randomly alternated until a total of five response reversal points were collected from both staircases. The six reversal points were averaged to give one value for the 50% detectability threshold for a double random staircase trial.

Following the recommendation of Perz et al. (2015) for obtaining the lowest variance and greatest sensitivity to stroboscopic effects presentations of modulated light were alternated with a dc reference presentation of the same time-average illuminance on 2-second intervals. Therefore, the subjects' task was to indicate whether the test condition was different than the dc reference condition. Between each alternating presentation the illumination would blink off briefly (roughly 100 ms), making it obvious to the subjects when the presentation had changed.

Subjects

Eight subjects, three female, participated in the study after signing informed consent forms approved by Rensselaer's Institutional Review Board. Ages ranged from 22 to 52 years with a mean of 33 years. The experiment took place in the Levin Photometric Laboratory at the Lighting Research Center, a black painted room, where the experimental apparatus described above was the only source of illumination. Subjects were seated 1.5 meters from the spinning disk and white background. A computer keyboard located to the side of the subject was used to record responses, down arrow if a stroboscopic contrast pattern was detected, up arrow if not detected. Every subject performed at least one double random staircase practice trial before starting their sequence of experimental conditions. The 40 waveform conditions were split into two sessions occurring one to three days apart. Each session required roughly one hour to complete. Within each session the order of waveform presentations were randomized. Each session contained eight sine-wave conditions and 12 randomly selected complex waveforms chosen without replacement from the list of complex waveforms being tested.

Results

Sinusoidal waveforms

Table 2 contains the threshold sinewave light modulation values (percent flicker) for detecting a stroboscopic contrast pattern on the spinning disk. Table 3 contains the corresponding calculated spatial contrast values for every threshold condition. These spatial contrast values were calculated by use of equation 6 after converting the light and object profile waveforms to the frequency domain via a Fourier transform. Because the light waveform is sinusoidal there is only one frequency component. Alternately, equation 3 could be used with the time domain signals to calculate the resulting spatial pattern, followed by the calculation of contrast using the formula Contrast = (max – min)/(max + min).

Table 2. Percent light modulation relative to mean light level (percent flicker) at threshold detection of a stroboscopic contrast pattern for every subject and trial along with the average for each sinewave frequency of the illumination waveform.

Sinewave frequency Hz	Sub 1	Sub 2	Sub 3	Sub 5	Sub 6	Sub 7	Sub 8	Sub 9	Average
60	6.27	9.44	3.95	10.98	5.74	9.17	11.07	7.13	8.68
60	5.07	7.16	4.73	9.19	17.81	8.40	8.84	13.99	
120	2.72	3.12	3.37	4.68	3.15	3.53	3.24	3.99	3.32
120	2.38	2.52	1.41	3.76	5.78	3.77	1.51	4.14	
240	1.37	1.33	1.12	3.01	1.21	1.91	1.07	1.24	1.53
240	1.29	1.29	1.34	2.61	1.44	1.63	0.85	1.77	
480	0.98	1.20	0.95	1.97	1.39	1.40	0.60	1.97	1.34
480	1.09	1.21	0.74	2.64	1.34	1.57	0.73	1.64	
720	2.00	2.28	3.47	4.48	1.65	2.61	1.74	2.86	2.51
720	1.78	1.53	1.69	3.83	2.83	2.40	2.46	2.59	
1380	3.97	4.12	6.01	9.45	6.59	4.68	7.10	6.01	6.23
1380	4.53	3.46	3.38	10.92	8.52	5.62	5.26	10.05	
2340	14.93	18.66	20.98	28.71	6.65	32.79	58.49	45.43	28.24
2340	14.64	14.16	29.10	38.86	31.57	28.60	38.23	30.04	
3300	42.19	40.82	99.00	87.35	54.00	93.13	258.75	70.41	82.31
3300	44.30	34.62	88.90	99.00	99.00	52.72	85.52	67.29	

Table 3. Percent spatial modulation (spatial contrast) of the spinning sector disk for every subject, trial and corresponding averages for the sinewave illumination waveforms.

Sinewave frequency Hz	Sub 1	Sub 2	Sub 3	Sub 5	Sub 6	Sub 7	Sub 8	Sub 9	Average
60	3.30	4.98	2.08	5.78	3.02	4.83	5.84	3.76	4.58
60	2.67	3.78	2.49	4.85	9.39	4.43	4.66	7.37	
120	1.40	1.61	1.73	2.41	1.62	1.82	1.67	2.06	1.71
120	1.23	1.30	0.73	1.94	2.97	1.94	0.77	2.13	
240	0.65	0.63	0.53	1.42	0.57	0.91	0.51	0.59	0.72
240	0.61	0.61	0.63	1.24	0.68	0.77	0.40	0.84	
480	0.33	0.40	0.32	0.65	0.46	0.46	0.20	0.65	0.44
480	0.36	0.40	0.24	0.87	0.44	0.52	0.24	0.54	
720	0.30	0.34	0.52	0.67	0.25	0.39	0.26	0.43	0.38
720	0.27	0.23	0.25	0.57	0.42	0.36	0.37	0.39	
1380	0.45	0.47	0.69	1.08	0.75	0.53	0.81	0.69	0.71
1380	0.52	0.40	0.39	1.25	0.97	0.64	0.60	1.15	
2340	1.01	1.27	1.42	1.95	0.45	2.22	3.97	3.08	1.91
2340	0.99	0.96	1.97	2.63	2.14	1.94	2.59	2.04	
3300	2.04	1.97	4.78	4.22	2.61	4.49	12.49	3.40	3.97
3300	2.14	1.67	4.29	4.78	4.78	2.54	4.13	3.25	

Figure 3 displays spatial contrast sensitivity functions (CSF) for every subject along with the average curve derived from the data in Table 3. To extend the range of spatial frequencies, which is important for later analyses and to aid with curve-fitting, two additional data points were added at 0.1 and 60 cycles/degree using values consistent with previously published CSF functions, e.g., Mannos and Sakrison (1974). Sixth-order polynomial curve-fits were calculated in log-space.

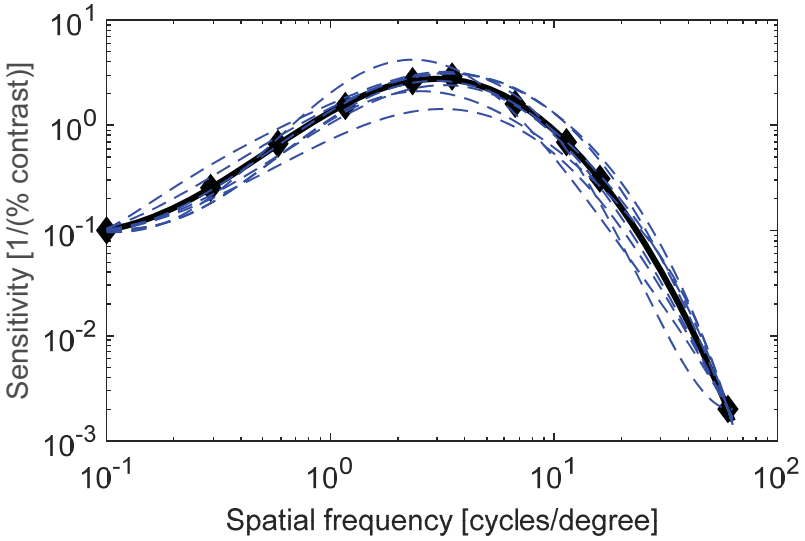

Figure 3. Spatial contrast sensitivity functions (CSF) determined for the eight subjects (dashed lines) and the average (solid line). Black diamonds mark the measurement points and anchor points (see text for details).

Non-sinusoidal waveforms

The light source modulation values for threshold detection of stroboscopic contrast for the non-sinusoidal temporal waveforms are listed in Table 4. Empty cells indicate missing data due to procedural errors. The visibility of the stroboscopic pattern for every experimental condition of waveform and frequency were calculated according to Equation 8 using the data of Table 4, the individual CSFs determined for each individual subject, and the physical dimensions and rotational speed of the spinning disk. These visibility values are listed in Table 5. The theoretical expected value for every condition is 1 because the light source modulation input values correspond to threshold detection.

Table 4. Percent light modulation relative to mean light output (percent flicker) at threshold detection of a stroboscopic contrast pattern for every subject and trial along with averages across subjects for the non-sinewave illumination waveform conditions.

Waveform type	Frequency (Hz)	Duty Cycle %	Sub 1	Sub 2	Sub 3	Sub 5	Sub 6	Sub 7	Sub 8	Sub 9	Average
Rectangular	60	20	2.35	2.78	1.96	3.54	2.51	1.78	2.63	2.35	**2.49**
Rectangular	120	10	1.32	1.72	1.85	3.55	2.11	1.30	1.74	2.34	**1.99**
Rectangular	120	20	1.45	1.29	1.25	2.82	2.00	1.42	0.92	1.65	**1.60**
Rectangular	120	50	1.90	1.98	1.78	3.19	2.38	2.20	1.11	2.57	**2.14**
Rectangular	240	20	1.36	1.56	1.36	2.37	1.77	1.33	1.02	2.07	**1.61**
Rectangular	420	10	2.83	4.88	1.91	4.84	3.70	2.24	2.44	3.90	**3.34**
Rectangular	420	50	1.09	3.98	0.71	1.58	2.42	1.08	0.71	1.33	**1.61**
Rectangular	480	20	1.41	1.42	1.41	2.28	1.49	1.91	2.42	1.67	**1.75**
Rectangular	720	20	2.24	2.99	2.34	5.72	2.34	4.55	4.86	3.04	**3.51**
Rectangular	1380	20	5.45	6.24	5.52	12.70	9.58	7.20	11.24	10.70	**8.58**
Rectangular	1500	10	9.30	12.07	21.80	23.88	17.23	16.45	20.30	22.44	**17.93**
Rectangular	1500	50	4.01	3.59	4.57	13.48	7.14	6.37	7.01	7.81	**6.75**
Rectangular	2340	20	14.95	17.84	24.55	32.89	27.47	30.34	60.69	46.35	**31.89**
Rectangular	3300	20		23.79		95.16	67.84	59.41		72.68	**63.77**
Rectified sine	100	--	3.42	5.60		7.56	5.56	3.32	5.89	7.86	**5.60**
Rectified sine	120	--	1.57	2.87	2.65	4.42	4.14	3.70	2.43	4.59	**3.30**
Rectified sine	420	--	1.22		0.91	3.03	1.63	1.34	0.93	1.79	**1.55**
Rectified sine	1500	--	22.46	3.46	5.82	15.80	12.29	9.59	8.24	12.67	**11.29**
Sawtooth	120	--	2.70	2.10	2.52	4.59	3.17	3.47	2.42	2.97	**2.99**
Sawtooth	420	--	1.68		1.53	3.44	2.40	1.55	1.20	2.72	**2.07**
Sawtooth	1500	--	5.00	9.44	17.85	17.67	10.73	13.86	13.11	12.33	**12.50**
Ramp (triangle)	120	--	3.12	2.46	2.55	5.58	2.85	4.94	2.49	6.36	**3.79**
Ramp (triangle)	420	--	1.71		0.99	2.14	1.80	1.42	0.97	2.05	**1.58**
Ramp (triangle)	1500	--	6.30	7.66	13.81	13.95	12.22	8.83	7.68	10.96	**10.18**

Table 5. Stroboscopic detection metric, $(\Sigma C_P^2)^{1/2}$, of the spinning sector disk at threshold detection of stroboscopic contrast patterns for every subject and trial along with averages across subjects for the non-sinewave illumination waveform conditions.

Waveform type	Frequency (Hz)	Duty Cycle %	Sub 1	Sub 2	Sub 3	Sub 5	Sub 6	Sub 7	Sub 8	Sub 9	Mean
Rectangular	60	20	1.098	1.206	1.028	0.861	0.909	0.599	1.599	0.777	**1.010**
Rectangular	120	10	0.765	0.963	1.203	1.030	1.032	0.573	1.493	0.992	**1.006**
Rectangular	120	20	0.994	0.845	0.960	0.994	1.132	0.723	0.927	0.840	**0.927**
Rectangular	120	50	1.229	1.188	1.280	1.062	1.188	1.024	0.926	1.175	**1.134**
Rectangular	240	20	1.118	1.239	1.249	0.963	1.230	0.837	1.244	1.243	**1.140**
Rectangular	420	10	1.164	0.642	0.858	0.958	1.303	0.714	1.473	1.144	**1.032**
Rectangular	420	50	1.360	1.269	0.985	0.940	2.580	1.056	1.349	1.194	**1.342**
Rectangular	480	20	0.995	0.963	1.114	0.756	0.891	1.056	2.495	0.820	**1.136**
Rectangular	720	20	0.878	1.129	0.904	0.989	0.721	1.333	1.956	0.714	**1.078**
Rectangular	1380	20	1.029	1.173	0.744	1.000	1.326	0.895	1.145	1.045	**1.045**
Rectangular	1500	10	0.803	1.073	1.432	0.938	1.130	0.966	0.926	1.078	**1.043**
Rectangular	1500	50	1.035	0.930	0.801	1.384	1.303	1.050	0.866	0.994	**1.045**
Rectangular	2340	20	0.767	0.988	0.716	0.789	1.072	1.026	1.517	1.487	**1.045**
Rectangular	3300	20		0.465		1.558	1.286	0.856		1.104	**1.054**
Rectified sine	100	--	0.538	0.490		0.374	0.405	0.225	0.738	0.529	**0.471**
Rectified sine	120	--	1.014	0.900	1.004	0.809	1.025	0.862	0.941	1.093	**0.952**
Rectified sine	420	--	1.004		0.845	1.188	1.148	0.865	1.167	1.059	**1.031**
Rectified sine	1500	--	0.200	0.594	0.669	1.036	1.448	1.027	0.663	1.039	**0.835**
Sawtooth	120	--	1.164	0.857	1.206	1.008	1.097	1.096	1.452	0.926	**1.101**
Sawtooth	420	--	1.048		1.073	1.028	1.287	0.759	1.140	1.221	**1.079**
Sawtooth	1500	--	0.646	1.226	1.565	0.907	0.980	1.143	0.809	0.785	**1.008**
Ramp (triangle)	120	--	0.973	0.690	0.871	0.930	0.627	1.030	0.823	1.356	**0.913**
Ramp (triangle)	420	--	1.348		0.877	0.807	1.220	0.881	1.171	1.165	**1.067**
Ramp (triangle)	1500	--	1.037	1.265	1.541	0.912	1.421	0.927	0.604	0.888	**1.074**
										Mean	**1.024**
										Std. error	**0.030**

Discussion

Contrast sensitivity

The directly measured threshold light source modulations in Table 2 must be convolved with the reflectance profile of the spinning disk in order to determine the spatial contrast stimulus viewed by the subjects. The resulting values of spatial contrast, displayed in Table 3, are always less than the percent flicker of the light source because 1) the reflectance contrast of the white

and black disk is less than one, and 2) the superposition of reflected light across the width of the spinning wedges increasingly fills-in the spatial pattern as the width of the wedges increase. Thinner wedges preserve the contrast in the temporal light signal at the expense of lower overall luminance of the spatial pattern.

The values of threshold spatial contrast reported in Table 3 are similar to those reported previously in literature regarding human visual sensitivity to sinewave gratings. Van Nes and Bouman (1967) measured threshold modulation curves for human vision at different retinal illuminance levels for monochromatic light. At 900 trolands, which corresponds roughly to the light level used in this experiment, their data show an ultimate detection limit of 0.2% contrast for green light (λ = 525 nm) at a spatial frequency of approximately 4 cycles/degree. The 4 cycles/degree maximum sensitivity agrees well with the CSFs shown in Figure 3, and the lowest measured spatial contrast (Table 3) is 0.23% which is just slightly above the reported ultimate detection limit.

Stroboscopic sensitivity predictions

Using the individual CSFs measured for each subject the mean stroboscopic visibility value for all subjects and waveform/frequency conditions is 1.026 with a standard deviation of 0.307. For the 184 threshold values the standard error of the mean is 0.0226. A histogram of the visibility values, Figure 4, shows a distribution that is well described by a normal probability distribution except for two outliers having values near 2.5. This visual judgement normality is supported by skew and kurtosis measures of 1.2 and 5.8, respectively, which drop to -0.004 and 0.97 when the two outliers are removed. A two-tailed Z-test including the outliers returns a probability of 0.25 for this sample coming from a distribution with a mean equal to 1. Therefore, there is no reliable evidence that the linear systems modeling of stroboscopic detection has systematic accuracy errors for predicting threshold. This result is robust given that the waveforms used to test the model were diverse with many, especially the short duty cycle rectangular waveforms, having large amounts of harmonic content. Moreover, the large amount of harmonic content in many of the waveforms provided for a sensitive test of whether the summation of spectral contrast components adheres to a Euclidean vector norm (exponent of 2 in Equation 8) or some other p-norm like that proposed in Perz et al. (2015) who report a best-fit value of p = 3.7. An explanation of why the analysis by Perz et al. led to a p-norm of 3.7 is the omission of taking into account the characteristics of their moving object for producing the stroboscopic effects; they only considered the light source temporal waveform and not the convolution of it with the moving object to fully specify the visual stimulus.

The average values across waveform types, row averages in Table 5, are also all very close to 1 except for the rectified sinewave at 100 Hz which has an average metric value of 0.47. A possible reason for this low value is that the time constant used to model the persistence of vision is not optimal. 100 Hz is not an integer multiple of the spinning disk frequency so too short of a time constant could reduce the perceived contrast by not allowing the signal to build-up enough, or too long could cause cancellation of the spatial pattern. This will need to be investigated further.

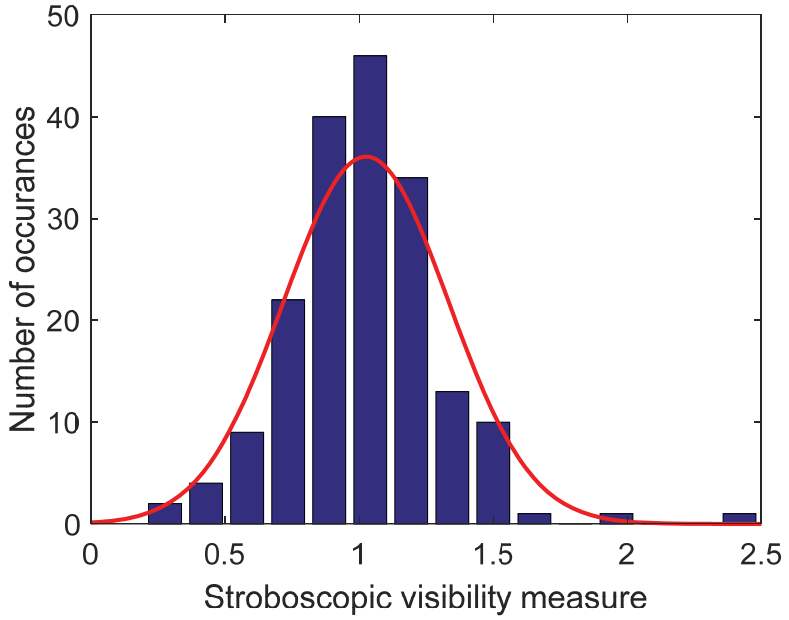

Figure 4. A histogram of stroboscopic visibility measures for all subjects and all non-sinusoidal waveform conditions (blue bars) plotted with a normal distribution (red line) having the same mean and standard deviation.

Predicting previous experimental outcomes

The Perz et al. study used a well-defined moving target to produce stroboscopic effects that can be easily applied to the present model. In their study a 26 mm diameter white spot on a black background revolved around a 200 mm diameter circular path at a linear speed of 4.0 m/s. The reflectance profile used for modeling was a 26 mm wide rectangular reflectance pulse ($\rho = 0.93$) spaced $200\times\pi$ mm apart along a black baseline ($\rho = 0.06$). Their study used square wave light modulation (rectangular waveform, 50% duty cycle) at frequencies of 50, 100, 200, and 400 Hz. Figure 5 shows the modeling results for threshold stroboscopic detection over a light source modulation frequency range from 30 Hz to 10 kHz. The following observations are made from the graph:

1) The lowest detectable modulation is roughly 4%. This is substantially greater than the limit for the spinning sector disk used in this study because the white reflectance profile of the Perz et al. is much wider than that of the spinning sector disk used in this study (2.1° vs 0.26°). The wider target results in a lower physical spatial contrast. Also, the spacing of the Perz et al. target (one per revolution) was greater than that for the sector disk (8 per revolution) leading to less reinforcement of the stimulus as it fades due to the exponential-like decay of the persistence of vision. These two factors, object size and repetition rate, can substantially raise the detection limit for stroboscopic effects.
2) Threshold amplitudes range from 4% to 50% depending on the modulated light frequency. The large oscillatory variation with frequency results from the interaction of the object size and speed with the timing of the modulated illuminating light. At certain frequencies (or object speeds) the object moves just enough between pulses of light to fill-in past revolutions of the stimulus thereby reducing the apparent time-averaged

contrast pattern. At other frequencies (or speeds) the stroboscopic pattern is reinforced each revolution. A similar interaction occurs between different object sizes and modulation frequency; certain size/frequency combinations reinforce the physical spatial pattern while others lead to cancellation of the patterns over time. The average threshold modulations for Perz et al. are indicated with filled circles with the error bars showing the range of individual trials. As an accurate model should predict, the entire range of results all lie above the modeled threshold line. Note that there is some uncertainty in the exact horizontal placement of the Perz et al. data points relative to the modeled results due to the viewing distance of 0.7 m being estimated from the published description of the apparatus.

3) The envelope of modulation threshold values stays fairly constant up to about 1 kHz, then rapidly increases to 100% (no amount of modulation is detectable). The reason for the sudden rise in threshold modulation is again due to the size and speed of the object. Eventually, as the frequency is increased the object does not move more than the distance of its width between pulses of light resulting in a loss of physical contrast. This explains why, in general, high modulation rates result in less objectionable flicker.

The detection of stroboscopic flicker caused by square wave modulated light was also investigated by Bullough et al. (2012). In that study subjects sat at a desk in a room illuminated by LED lights producing controlled amounts of square wave light modulation. Subjects were given a white 12-inch ruler which they could wave back and forth in a manner they deemed best for detecting stroboscopic effects. Since the exact speed and angle of the ruler movement is unknown the modeling results were obtained by using a range of object profiles corresponding to holding the ruler at different angles, and by using a range of waving speeds attainable by hand movements (1 to 5 m/s). Model calculations were made over the range of light source modulation frequencies and modulation amounts used in Bullough et al. and the minimum modulation detection threshold values were used from each speed and object profile model run to develop the contour plot shown in Figure 6 shown with the original plot from Bullough et al. (2012).

The 40-60% detection contour interval of Bullough et al. is comparable to the stroboscopic visibility measure of 1 as both can be considered a threshold value. Note the general shape of the contours are similar with sensitivity greatly diminishing for frequencies above 3 kHz and the lowest detectable modulation being approximately 5%. The model also reproduces the slight decrease in sensitivity for low frequency modulation below approximately 250 Hz.

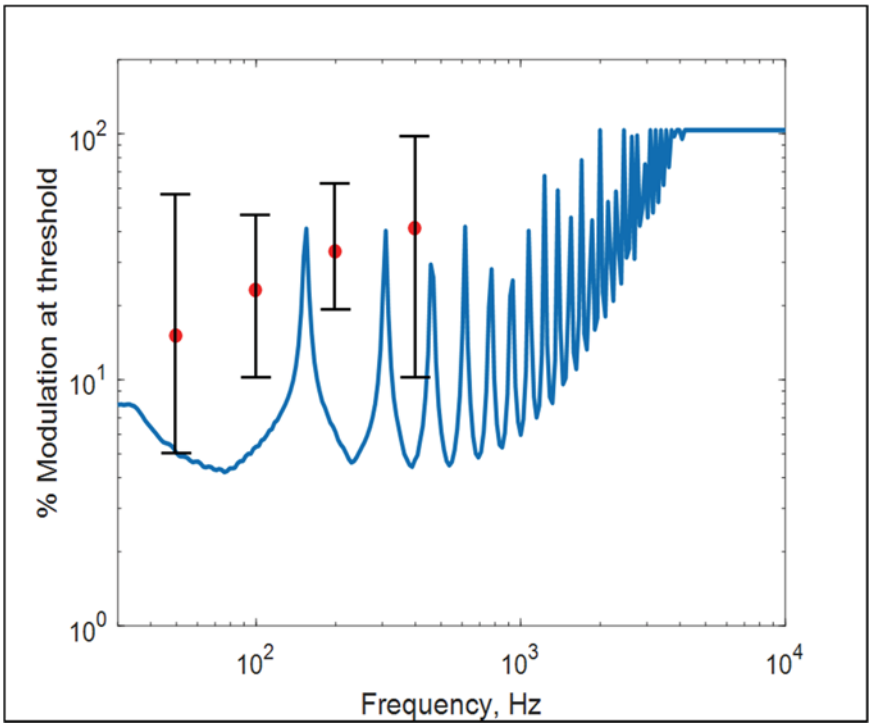

Figure 5. Threshold light source square wave modulation (percent flicker) for detecting stroboscopic effects for conditions similar to those used in the Perz et al. study: a 26 mm white rectangle spaced 628 mm apart (arc distance for radius = 100 mm) moving at 5.71 radian/s (4.0 m/s @ 0.7 m viewing distance). Round symbols mark the approximate mean threshold values reported by Perz et al. with error bars showing the range of responses.

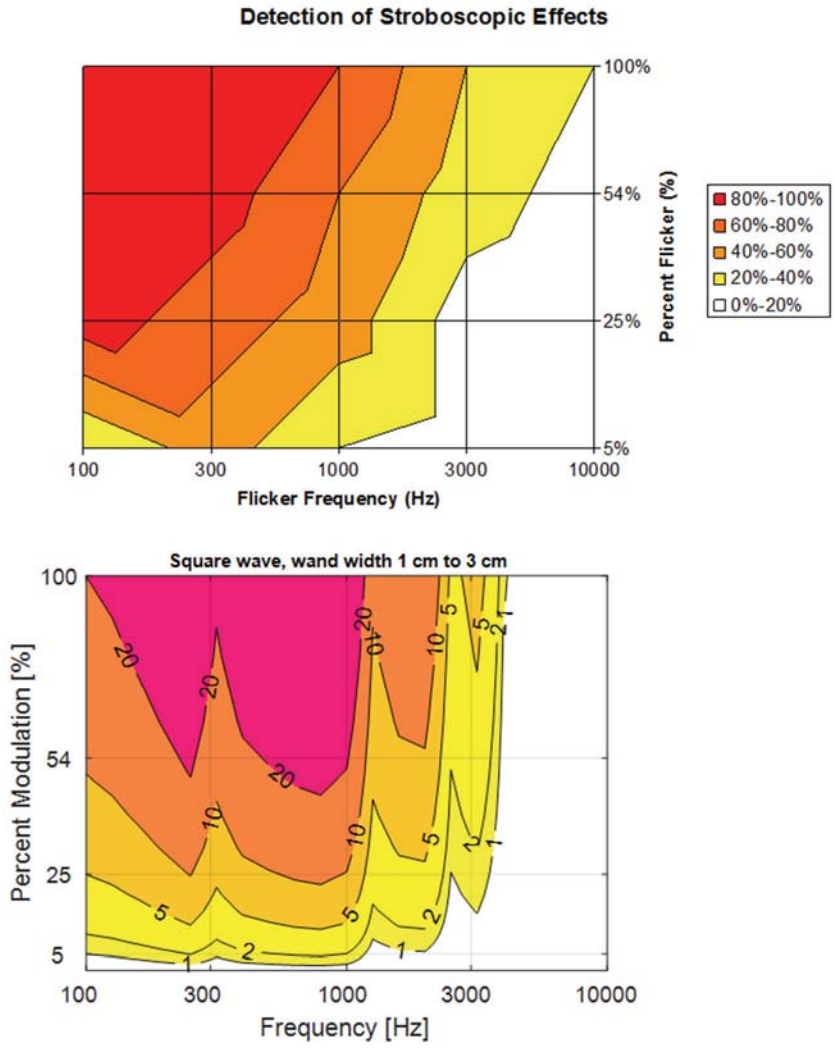

Figure 6. Comparison of model predictions (bottom) to experimental results (top) for the detection of stroboscopic effects. Contours for the top graph show detection rates. Contours on bottom graph show multiples of the stroboscopic visibility measure where a value of 1 is threshold and can be regarded as the 50% detection rate.

Ultimate stroboscopic detection

As shown by modeling, detection of stroboscopic effects is strongly dependent on the object profile and speed. Is there an object profile and speed that are optimal for detecting stroboscopic effects? The answer is yes and the values are found by considering the CSF. The maximum contrast sensitivity for the subjects in this study occurs at approximately 3.5 cycles/degree = 200 cycles/radian. An object profile half this visual angle will therefore produce maximum contrast. Therefore, the optimum moving object width, w_O, is given by:

$$w_O = \frac{1}{2f_{max}} \text{ [radians]}, \qquad \text{Equation 9}$$

where f_{max} is the frequency (cycles/radian) of the CSF where sensitivity is maximum. For humans w_O is approximately 0.0025 radians. At a viewing distance of 1 meter this corresponds to a 2.5 mm thick stick.

The frequency of modulation that produces the highest physical contrast is dependent on the speed and the width of the moving object. This frequency occurs when the object moves exactly two object widths during the period of light modulation. In equation form,

$$v_O = 2w_O\omega_L/2\pi = w_O\omega_L/\pi \text{ [radians/s]} \qquad \text{Equation 10}$$

where v_O is the velocity of the object expressed in visual angle (radians/s), and ω_L is the frequency of light modulation. For example, v_O = 0.5 m/s for a 100 Hz waveform and an object at 1 meter distance.

Running the stroboscopic visibility model for different light output waveforms using the optimal object size and optimal speeds results in a constant modulation threshold across all light frequencies. The constant changes for different waveform shapes and so different light output waveforms can be rank-ordered for their potential for producing detectable stroboscopic flicker. Figure 7 plots the model output for several waveforms. When producing Figure 7 an upper limit was placed on object speed corresponding to the maximum human eye saccade of 900 degrees/s. With the upper limit on object speed the modulation thresholds show the expected trend of decreasing sensitivity to stroboscopic flicker as frequency increases. However, before the speed limit is reached sensitivity to stroboscopic flicker is not dependent on light source frequency if the speed of the object is variable.

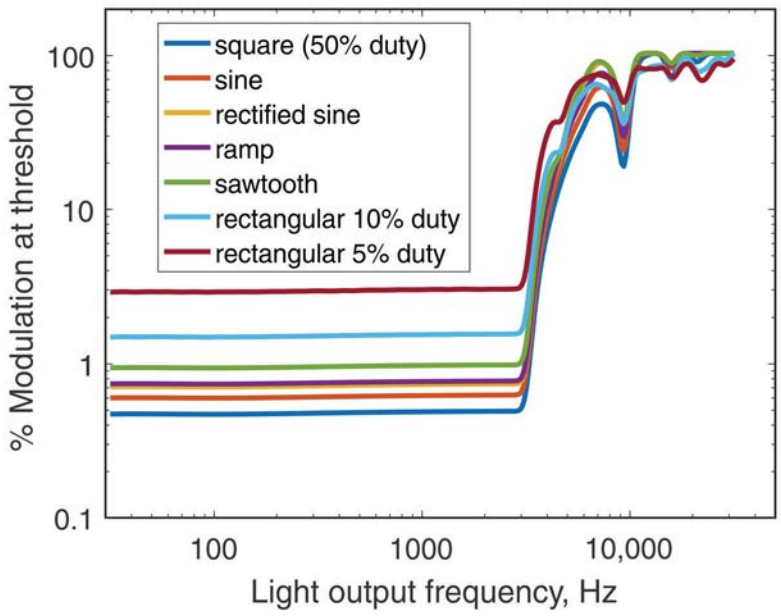

Figure 7. Light source modulation at the threshold of detection of stroboscopic effects for optimal object size and speed for different light waveforms as a function of light output frequency. The object speed was limited to the fastest human eye saccade.

Extending detection to acceptability

While an accurate model for predicting stroboscopic detection is useful for evaluating particular lighting situations where the viewing conditions can be well characterized in terms of object profiles and speeds, by itself it is not very useful for determining the acceptability of a light source for general use. As shown, the ultimate modulation detection thresholds are so low that

practically all ac operated electric lights have detectable flicker. As shown by Bullough et al. (2012), however, a light source can be acceptable for illumination even though under particular circumstances it produces stroboscopic flicker. While acceptability is difficult to predict for the general case, it can be empirically measured for specific cases. Assuming that acceptability is ultimately dependent on detection, that is, less acceptable light sources have more readily detectable flicker, acceptability results for one type of waveform can be extended to any other arbitrary waveform by using the ratios of stroboscopic detection to determine acceptability. A procedure for doing this is described below.

The acceptability of perceived stroboscopic effects produced under square-wave modulation of varying modulation depths (% flicker) was empirically modeled by Bullough et al. Acceptability, a, was given by:

$$a = 2 - \frac{4}{1+\frac{f}{130log_{10}(p)-73}} \qquad \text{Equation 11}$$

Where f is the dominant frequency of modulation (typically the fundamental frequency of a periodic waveform) and p is percent flicker. The numerical values of a are interpreted as follows:

+2	very acceptable
+1	somewhat acceptable
0	neither acceptable nor unacceptable
-1	somewhat unacceptable
-2	very unacceptable

Presumably, subjects' acceptability responses are related to how easily flicker-manifested contrast is detected; the higher the detection probability the lower the acceptability. This is roughly supported by the contour plots of detection and acceptability versus frequency and percent flicker of Bullough et al. The detection of flicker-manifested contrast is known to depend on the shape of the light waveform, so it is likely that acceptability also depends on wave shape. A method for extending the acceptability formula, generated using square-wave modulation, to all possible light waveform types is to scale percent flicker, p, by the ratio of perceptible modulation for the waveform in question to that for a square wave. Essentially, what originally was percent flicker that merely describes the amplitude variation of the waveform is now replaced by a measure of perceptual flicker that accounts for wave shape and which is normalized to square-wave equivalent values for use in the Bullough et al. formula:

$$a = 2 - \frac{4}{1+\frac{f}{130log_{10}(p_P)-73}} \qquad \text{Equation 12}$$

where

$$p_P = p\frac{C_P(DUT)}{C_P(squarewave,f_{DUT},p_{DUT})} \qquad \text{Equation 13}$$

C_P is the perceptual stroboscopic contrast and it is calculated by using the optimum object size and speed in Equation 8. The calculation requires a relative light output waveform as a function

of time for the device under test (DUT). C_P is independent of the frequency of the light waveform unless an upper limit is placed on the speed of objects. No upper speed limit is used for determining the C_P ratio because the formula for acceptability already includes a dependency on frequency which was determined by the conditions used in the studies leading to the acceptability ratings. The ratio of C_P values, therefore, is only dependent on the light waveform, and so a simple table of p multipliers can be generated for different waveforms. Table 6 lists p multipliers for wave shapes used in this study.

Table 6. Perceptual contrast ratios for different waveforms. In each case the perceptible contrast, C_P, of the device under test (DUT) is divided by the C_P of a square wave having the same percent flicker.

Waveform	C_P ratio (DUT/square)
Square	1.00
Sine	0.78
Rectified sine	0.66
Ramp	0.64
Rectangular 20% duty cycle	0.59
Rectangular 80% duty cycle	0.59
Sawtooth	0.50
Rectangular 10% duty cycle	0.31

For an example of the procedure, say one wants to calculate an acceptability rating for a 400 Hz rectified sinewave at 20% modulation.

The C_P ratio of a rectified sinewave is 0.66. Multiplying this by the rectified sinewave modulation gives the perceptual modulation for this waveform.

$$p_P = p \times (C_P ratio) = 20\% \times 0.66 = 13.2\% \qquad \text{Equation 14}$$

$$a = 2 - \frac{4}{1+\frac{f}{130log_{10}(p_P)-73}} = 2 - \frac{4}{1+\frac{400}{130log_{10}(13.2)-73}} = 1.385 \qquad \text{Equation 15}$$

For comparison, a 400 Hz square wave at 20% modulation gives a = 1.225.

Conclusions

A linear systems approach was used to model the human detection of stroboscopic flicker caused by the interaction of light output modulation and the size and speed of reflective, or self-luminous objects. An experiment enlisting the participation of eight subjects was conducted to verify the accuracy of the model. Model results were then compared to other published data on the detection of stroboscopic effects. Finally, through insights gained by the modeling, a procedure is proposed for using detectability results from the model to extend the usefulness of acceptability data on light source modulation limits to waveforms of all different types.

The following conclusions are made:

1. Linear systems modeling predicts well the detection of stroboscopic flicker. The modeled predictions are well within the uncertainty limits of the psychophysical method used to determine threshold.
2. The importance of including the reflectance profile and the speed of objects being viewed for accurate predictions of stroboscopic flicker has been demonstrated. The first step for modeling the stroboscopic effect is to model the physical spatial contrast pattern that is produced by the interaction of temporal light changes with the movement of objects.
3. The spatial contrast sensitivity function (CSF) weights the physical spatial contrast pattern frequency components to arrive at a measure of perceptual effectiveness.
4. Spectral components add as vectors in Euclidean space (exponent of 2 and square root used in Equation 8).
5. The ultimate detection of stroboscopic effects using an optimal sized object and optimum speeds is independent of waveform frequency. Therefore, different wave shapes can be rank-ordered for their flicker potential when equated for percent flicker.
6. Modeling flicker potential using optimal object size and speeds enables the limited amount of data available on light source stroboscopic flicker acceptability to be extended to light output waveforms of any shape.

References

ASSIST (2015). Recommended Metric for Assessing the Direct Perception of Light Source Flicker. Troy, New York: Lighting Research Center, Rensselaer Polytechnic Institute.

Bullough, J., K. S. Hickcox, T. Klein, A. Lok, et al. (2012). Detection and acceptability of stroboscopic effects from flicker. *Lighting Research & Technology* **44**: 477-483.

Cornsweet, T. N. (1962). The staircase-method in psychophysics. *The American Journal of Psychology* **75**: 485-491.

Eastman, A. A. and J. H. Campbell (1952). Stroboscopic and flicker effects from fluorescent lamps. *Illuminating Engineering* **47**: 27-35.

IEEE (2010). Recommended Practice—Adoption of IEC 61000-4-15:2010, Electromagnetic compatibility (EMC) —Testing and measurement techniques—Flickermeter—Functional and design specifications; Standard 1453-2011.

IEEE (2015). Recommended Practices for Modulating Current in High-Brightness LEDs for Mitigating Health Risks to Viewers; Standard 1789-2015.

Ku, S., D. Lu and P. Chen (2015). Predicting the stroboscopic effects of measured and artificial flicker waveforms through simulation. *Lighting Research & Technology* **47**: 1010-1016.

Mannos, J. and D. Sakrison (1974). The effects of a visual fidelity criterion of the encoding of images. *IEEE Transactions on Information Theory* **20**: 525-536.

NEMA (2017). Temporal Light Artifacts: Test Methods and Guidance for Acceptance Criteria; Standard NEMA 77-2017.

Olzak, L.A. and J. P. Thomas (1985). Seeing spatial patterns. In K. Boff, et al. (Eds.), *Handbook of perception and human performance*. New York: Wiley. pp. 7:1-56.

Perz, M., I. Vogels, D. Sekulovski, L. Wang, et al. (2015). Modeling the visibility of the stroboscopic effect occurring in temporally modulated light systems. *Lighting Research & Technology* **47**: 281-300.

Van Nes, F. L. and M. A. Bouman (1967). Spatial modulation transfer in the human eye. *JOSA* **57**: 401-406.